DOI 10.1515/htmp-2013-0042 — High Temp. Mater. Proc. 2014; 33(2): 161–170

Sare Çelik* and Ismail Ersozlu

Investigation of Microstructure and Mechanical Properties of Friction Welded AISI 316 and Ck 45 Steels

Abstract: This study has arisen from the necessity to manufacture an impeller and a shaft pair of a water pump from two different types of steels. The impeller has to have resistant to corrosion and the shaft has to have magnetic permeability property. It is deemed suitable to use the AISI 316 austenitic stainless steel performing high resistance corrosion for the impeller and Ck 45 carbon steel with magnetic permeability property for the shaft. The joining of AISI 316 and Ck 45 steels has been achieved by using the friction welding method. After welding process, the tests of tensile and micro hardness were applied, the microstructures were observed, and composition of elements was found in the welding zone. As optimum welding parameters, 100 MPa of friction pressure, 10 s of friction time, 200 MPa of upset pressure and 20 s of upset time were determined in 3000 rev/min rotation speed.

Keywords: friction welding, mechanical testing, microstructure, AISI 316 and Ck 45 steels

***Corresponding author: Sare Çelik:** Department of Mechanical Engineering, Faculty of Engineering and Architecture, Balikesir University, 10145 Balikesir, Turkey. E-mail: scelik@balikesir.edu.tr
Ismail Ersozlu: Department of Mechanical Engineering, Army Academy, 06100 Ankara, Turkey

1 Introduction

Friction welding is the solid state welding method avoiding fusion on the welded area and it is applied through using the heat caused by friction created entirely by the mechanical motion on the surfaces of parts without using the electrical energy or other energy sources [1, 2]. In the friction welding, the surfaces exposed to friction during welding process remain under axial pressure whereas this process named as the friction phase continues until the plastic deformation heat occurs [3, 4]. The upset is formed by stopping the rotating movement in this heat and increasing the axial pressure. Therefore, the welding area is exposed to a kind of thermo mechanical process and consequently the grain structure is not deformed in the jointing part [5, 6]. The friction welding is considered as the method to be used in joining of metals with different welding, thermal and mechanical characteristics since the jointing of material pairs, which are failed to be connected with the other welding methods due to the works under the fusion heat and the short welding time in the friction welding, provides energy and material savings.

In the welding area exposed to the friction welding a materials-transition region exists as well as the heat affected zones (HAZ) of the two main materials around this region. In the transition region of the materials, it is seen the atoms of both materials are exposed to diffusion mutually. If any mixing or twisting incident happens in this section mechanically, then the diffusion condition occurs in a wider area. The hot torsion occurred in the jointing during the braking and upset period also assists the reduction of grain size. The high cooling rate in the welding seam section might cause the formation of martensite in the steels exposed to transformation hardness [5].

The conducted analyses indicate the most effective parameters on the friction welding method requiring optimization are the friction time (t_s), friction pressure (P_s), upset time (t_u), upset pressure (P_u) and rotation time (n). On the other hand, the parameters such as sample geometry, thermal capacity of the material, transformation capacity of the material and the shortening rate in the height of parts (Δl) are also effective in joining [3, 7, 8].

In the literature, broad studies have been conducted on the friction welding of similar or dissimilar materials [9–13]. The friction welding analyses are performed for the AISI 304 stainless steel whereas the impact of welding parameters on the mechanical characteristics, welding seam and the area exposed to heat have been investigated [14–19]. The second most popular steel of the stainless steel class is the AISI 316 steel. This steel has the consumption rate of 20% in all manufactured stainless steel products. The AISI 316 steel has the oxidation resistance to 1143 K in the disrupted operations and to 1198 K in the continuous operations [20, 21]. Akbarimousavi and Gohari

Kia conducted the study regarding the mechanical characteristics and the changes in microstructure of the AISI 316L stainless steel together with the friction based Cp titanium [22]. Imran Bhamji and colleagues have worked on the linear friction welding of the AISI 316 steel [23]. However, another study is no found regarding the friction welding parameters of AISI 316 stainless steel and Ck 45 carbon steel having the common areas of usage and the effects on the welding structure.

This study has arisen from the need of manufacturing a water pump resistant to corrosion and longer operating life. Manufacturing an impeller resistant to corrosion, forming the pump part exposed to water with the material resistant to corrosion and manufacturing a shaft part with the magnetic permeability makes rotate the impeller (for the electric motor) caused the necessity to manufacture the impeller-shaft pair from two different steels. It is deemed suitable to use the AISI 316 austenitic stainless steel performing high resistance to corrosion for the impeller and the Ck 45 carbon steel with the magnetic permeability for the shaft. The joining of AISI 316 stainless steel and Ck 45 carbon steel has been achieved by using the friction welding method. The welding strength has been tested through applying the tensile test, microhardness test, macro and microstructure test of welded samples as well as the EDS analysis whereas the suitable welding parameters have been determined.

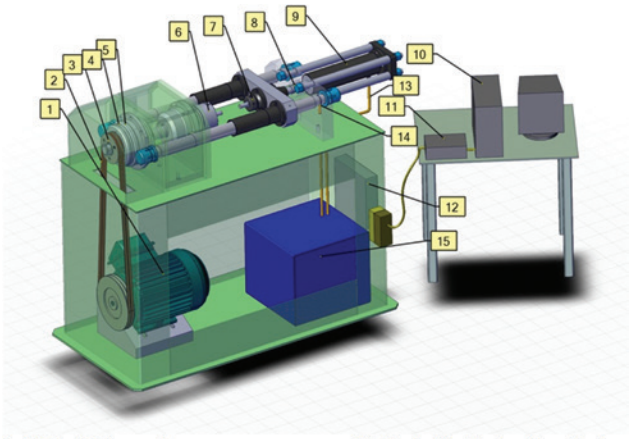

Fig. 1: The friction welding machine

2 Experimental procedure

Constant driving friction welding machine controlled by the computer with a maximum upset load capacity of 101,736 kN was used for implementing experimental study (Fig. 1). Samples of steel, which are 10 mm in diameter and 80 mm in length, were used in the experimental studies. The chemical analysis and mechanical tests of AISI 316 and Ck 45 steels have been conducted whereas the obtained results have been provided in Table 1 and Table 2 respectively. In these experimental studies, the constant drive welding machine has been used.

The grinding and polishing have been performed after the samples are processed with cutter horizontally for the optical and the Field Emission Scanning Electron Microscope (FESEM) microstructure analysis. Following the polishing process, the AISI 316 steel has been etched by electrolytic-etching through applying 15 volts and 1.5 ampere current for 10 g of $H_2C_2O_4$ (oxalic acid) + 100 mL H_2O (water) solution for 120 seconds [21]. On the other hand, the Ck 45 steel has been etched by holding 2% of HNO_3 (nitric acid) + 98% of methyl alcohol for 10 seconds in the etching device.

The Ck 45 steel side of welded samples has been etched first and the microstructures are analyzed and consequently the AISI 316 steel side has been etched and the Energy Dispersive Spectroscopy (EDS) analysis have been conducted following the application of re-polishing process of the welded samples.

The tensile tests have been prepared in accordance with the standards of EN 895 whereas the tests have been

Table 2: Mechanical properties of the AISI 316 and Ck 45 steels

Mechanical properties	AISI 316	Ck 45
Tensile strength (MPa)	663.55	715.2
Hardness (HV)	218	222

Table 1: The chemical composition of the AISI 316 and Ck 45 steels (mass%)

Material	%C	%P	%S	%Mn	%Si	%Mo	%Cr	%Ni
AISI 316	0.032	–	0.018	1.464	0.378	2.098	17.06	10.63
Ck 45	0.39	0.026	0.009	0.646	0.212	0.033	0.213	0.113

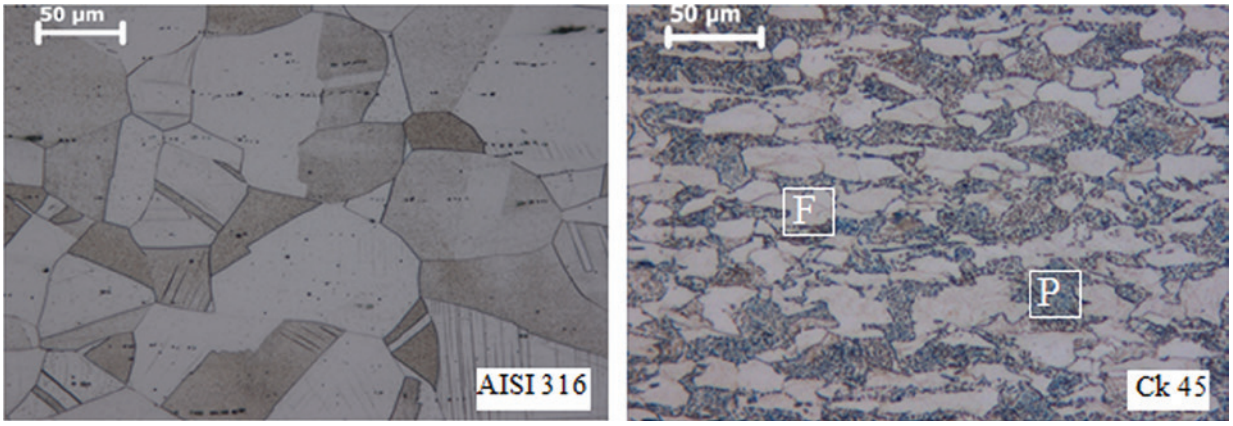

Fig. 2: Optical microstructure of AISI 316 (austenit) and Ck 45 steels (F: ferrite, P: pearlite)

performed at the rate of 2 mm/min in the tension device branded "Instron Corporation".

For the tensile measurement, the welded samples have been cut with a cutter and the sample surfaces have been cleaned by methyl alcohol following the grinding and polishing processes. The load of 50 g has been applied in the microhardness test for 20 seconds and the HV (Vickers) hardness has been measured.

Before the welding, the grain structure has been determined by conducting the optical microstructure investigation for the AISI 316 and Ck 45 steels whereas the results have been provided in Figure 2. The twin boundaries are seen in the microstructure of AISI 316 steel [21].

By considering the friction welding parameters obtained in the literature study [16–18] and the friction welding results of AISI 316 steel conducted as preliminary study, the jointing works of friction welding are performed for the AISI 316 and Ck 45 steels. The upset time (t_u) is set for 20 s and the rotational speed is set in 3000 rev/min whereas the other parameters are selected in the way indicated in Table 3.

Table 3: The friction welding parameters of the AISI 316 and Ck 45 steels

Sample no.	t_s (s)	P_s (MPa)	P_u (MPa)
1	8	80	160
2	8	80	200
3	10	80	160
4	10	80	200
5	6	100	120
6	6	100	160
7	6	100	200
8	8	100	120
9	8	100	160
10	8	100	200
11	10	100	120
12	10	100	160
13	10	100	200
14	6	120	120
15	6	120	160
16	6	120	200
17	8	120	120
18	8	120	160
19	8	120	200

3 Results and discussion

By the determined welding parameters, the AISI 316 and Ck 45 steels have been welded successfully through applying the friction welding method. The picture of welded sample is seen in Figure 3. Following the welding process, the realized shortening amounts in height are detected together with the diameter and width of flash occurred in the sides of both materials.

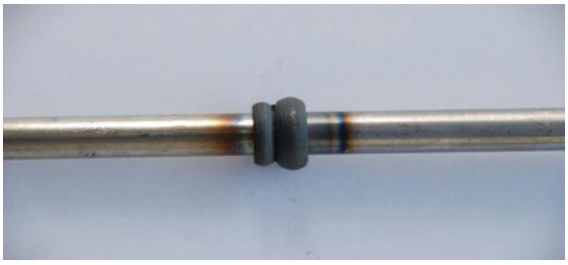

Fig. 3: The macroscopic view of welded

3.1 Microstructure Investigation

The optical and (FESEM) microstructure investigation of welded samples has been conducted. EDS analysis have been applied for the welded samples deemed suitable following the microstructure investigation.

By obtaining the general optical microstructure image of both materials (25×) in the welded sample 2, the information regarding the microstructures has been achieved (Figure 4). Consequently, the detailed optical microstructure investigation in the 6 sections (sections A, B, C, D, E and F) shown in Figure 5 has been performed for every welded starting from the main material side of Ck 45 steel towards the main material side of AISI 316 steel respectively (Figure 6). The etching solution of the AISI 316 steel has affected negatively the Ck 45 steel including the material transitions in the welded areas whereas this condition is observed in blackouts on the microstructure images of section D of Figure 5. During the microstructure investigation, the HAZ width of both materials has also been measured (Table 4).

By the optical microstructure analysis of welded samples, the FESEM investigation has been applied for the welded samples deemed suitable. In accordance with the optical microstructure investigation, the FESEM investigation has been applied for the welded samples in the sections given in Figure 9 starting from the main material of Ck 45 steel towards the HAZ of Ck 45 steel and the welding interface as well as the HAZ of AISI 316 steel and the main material of AISI 316 steel (Figure 7).

The welding section and HAZ have been analyzed by the optical microstructure and FESEM images of the welded samples. It is observed the materials are mixed through transition in the welding sections. The shape and depth of this mixture change in accordance with the welding parameters.

In the microstructure investigation applied for the Ck 45 steel side, the formation of martensite structure has

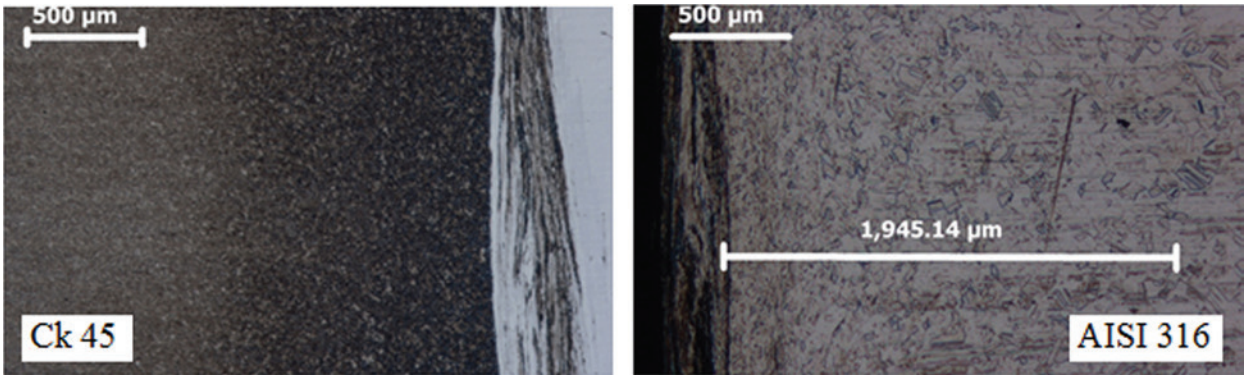

Fig. 4: Optical microstructure of welded Ck 45 and AISI 316 steels of sample 2

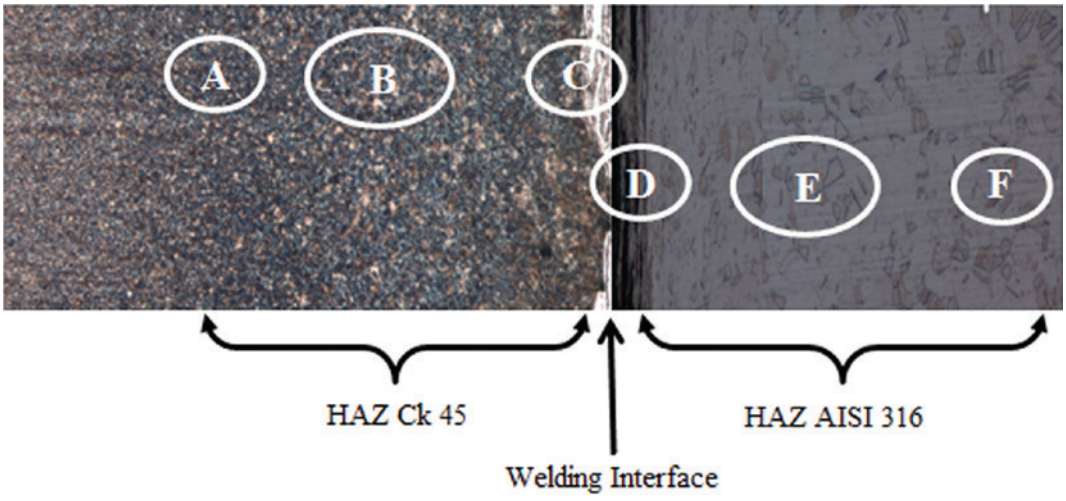

Fig. 5: Different zones of microstructure in the welded sample (25×)

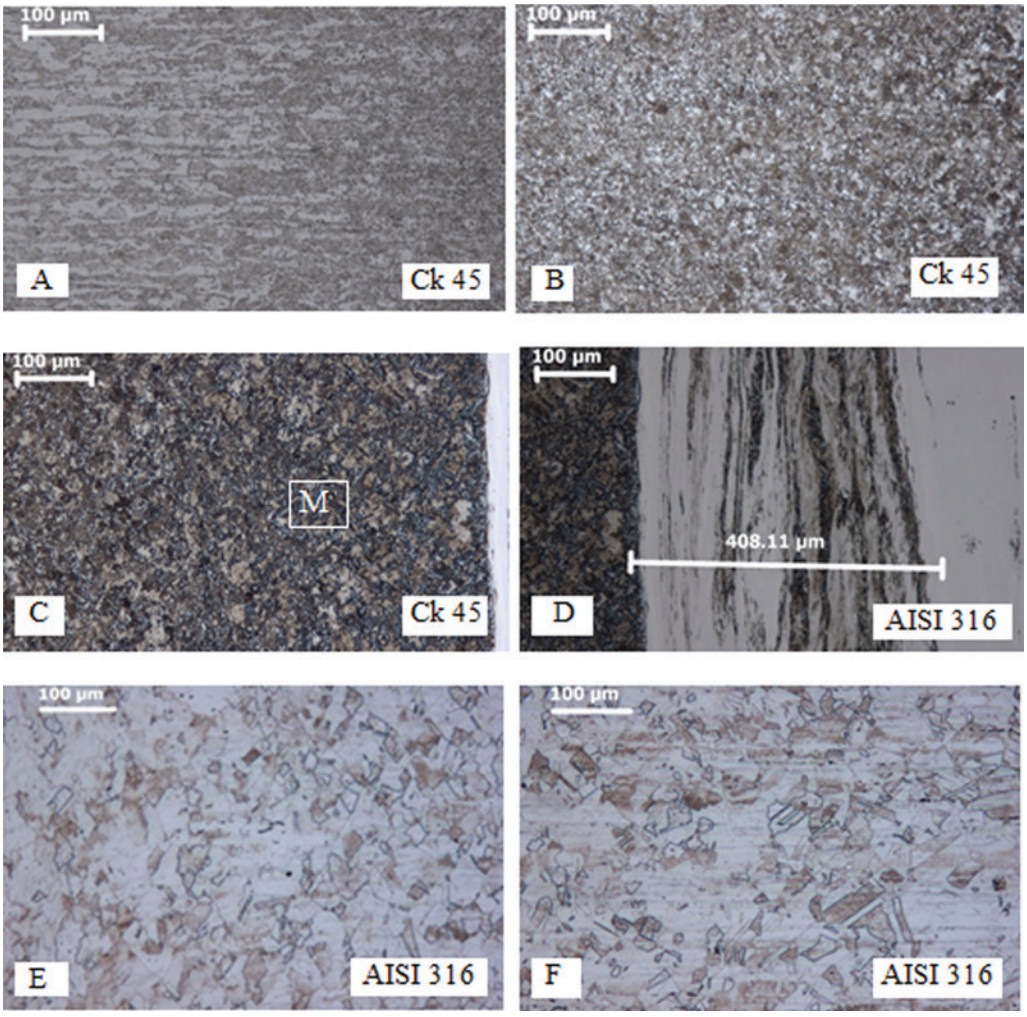

Fig. 6: Optical microstructures of welded sample in the different zones (M: martenzite)

been observed in the areas close to the welding interface (Figure 5, Section C). Towards the main material, the large grain structure and small grain structure have been observed respectively (Figure 5, Section B) whereas it is realized the main material returns to the initial grain size following a certain range (Figure 5, Section A).

In the microstructure investigation conducted in the AISI 316 steel, it is realized the dynamic re-crystallization in the HAZ and the new grain structures occur [14, 24]. From the welding interface towards the AISI 316 steel, the size of new grains changes in accordance with the deformation (axial pressure and rotation movement) and heat (Figure 5, Section D). Furthermore, it is observed the orientation has been realized from the center towards the vicinity. From this section towards the main material (Figure 5, Section E), the grain structure has grown in accordance with the reduced heat and deformation whereas it is realized the main material achieves the initial grain structure and size following a certain range (Figure 5, Section F) [20]. The HAZ width of both materials changes with regard to the welding parameters (Table 4). The HAZ width of welded samples occurred in the Ck 45 steel side is realized 1.73 times more than the HAZ width of AISI 316 steel in average. The increase rate of HAZ width of Ck 45 steel with regard to the HAZ width of AISI 316 steel has been reduced since the shortening rate realized in the height of Ck 45 steel is higher than the AISI 316 steel. The reason for this condition is that the amount of heated material in Ck 45 steel occurs as flash in the welding interface rather than the AISI 316 steel.

Following the FESEM investigation, the EDS analysis has been conducted for the welded samples. In accordance with the optical and FESEM microstructure investigations, the EDS analysis have been performed in the sections and the points shown in Figure 8 and determined for Sample 13 from the main material towards the welding

Table 4: Heat affected zone (HAZ) width of welded samples

Sample no.	HAZ width	
	AISI 316 steel (μm)	Ck 45 steel (μm)
1	2,873	4,000
2	1,945	2,900
3	2,005	3,914
4	2,571	3,245
5	1,990	3,475
6	2,639	2,969
7	2,215	2,618
8	1,956	3,574
9	1,615	3,587
10	1,853	3,000
11	1,682	4,065
12	1,223	3,420
13	2,200	3,032
14	2,476	2,938
15	2,031	2,960
16	1,518	2,842
17	1,682	3,480
18	2,143	2,933
19	1,312	3,356

interface. The results of EDS analysis are also provided in Table 5 and Table 6.

In the EDS analyses of welded samples, the element transitions are observed in the areas closer to the welding interface as well as on the welding interface. The mixture amount in both materials formed on the welding interface has increased this element transition. The Fe rate has decreased in the Ck 45 steel side whereas the Cr, Ni and Mo rates have been increased. On the other hand, the Fe rate has increased in the AISI 316 steel side whereas the Cr, Ni and Mo rates have decreased.

3.2 Mechanical properties

3.2.1 Tensile test

The picture of fractured surface following the tensile test is shown in Figure 9 whereas the results of tensile test applied for the welded samples are provided in Figure 10. Three tensile tests have been performed for every welding sample and the average value has been obtained. The lowest strength rates are seen in samples 5, 8 and 11 (Figure 10). In the analysis of welding parameters for the stated samples, the upset pressure of 120 MPa stands as the lowest rate. In the remaining samples 6, 9, 14, 15, 17 and 18 with the low tensile strength, the upset pressure is realized as 120 MPa and 160 MPa. On the other hand, the tensile strength of samples associated with the upset pressure of 200 MPa is rather higher.

In the results of tensile tests applied for the welded samples, the lowest tensile strength is seen as 192.9 MPa in sample 8 whereas the highest tensile strength is seen as 702.15 MPa in sample 13. Considering the lowest tensile strength rate, 64.4% less tensile strength is observed for the main material (AISI 316: 663.53 MPa) whereas 5.8% more tensile strength is achieved in consideration of the highest tensile strength rate. The welding parameters of Sample 13 are the optimum welding parameters as 3000 rev/mim with the 100 MPa friction pressure and 10 s of friction time, 200 MPa upset pressure and 20 s of upset time.

Following the tensile test, the fracture places and surfaces have been investigated. FESEM view of the fracture surface of sample 13 and 8 are given in Figure 11. By the macro investigation and the FESEM images of fracture surfaces, it is realized the fracture is brittle in most of the samples. The contraction of sections is observed partially in Sample 4 and 13. In the FESEM investigation of fracture surface of sample 13, the fracture is observed as ductile (Figure 11a). Brittle fracture and cracks have been observed in the analysis of fracture surface with FESEM of sample 8 which has low tensile strengh (Figure 11b). The structure of fracture surfaces changes in accordance with the welding parameters.

3.2.2 Microhardness test

The microhardness changes of the welded samples have been measured. The hardness values of selected samples obtained from the welded interface in horizontal position towards the sides of both materials have been provided in graphics in Figure 12. The tensile measurement signs have been given in Figure 13. From the welding interface towards the Ck 45 steel, the hardness value showed rapid increase within first 1 mm range whereas this increase showed a decreasing tendency within 1 and 2.5 mm and reached to the hardness value of Ck 45 steel. In the microstructure investigation of Ck 45 steel, it is observed the martensite structure is formed in the areas close to the welding interface whereas the large grain structure and the small grain structure is formed respectively while directed towards the main material whereas the main material achieves the grain size again following a certain range. This condition stands in parallel with the hardness distribution. From the welding interface towards the AISI 316 steel side, it is observed the hardness value remains unchanged in general. On the other hand, it is considered

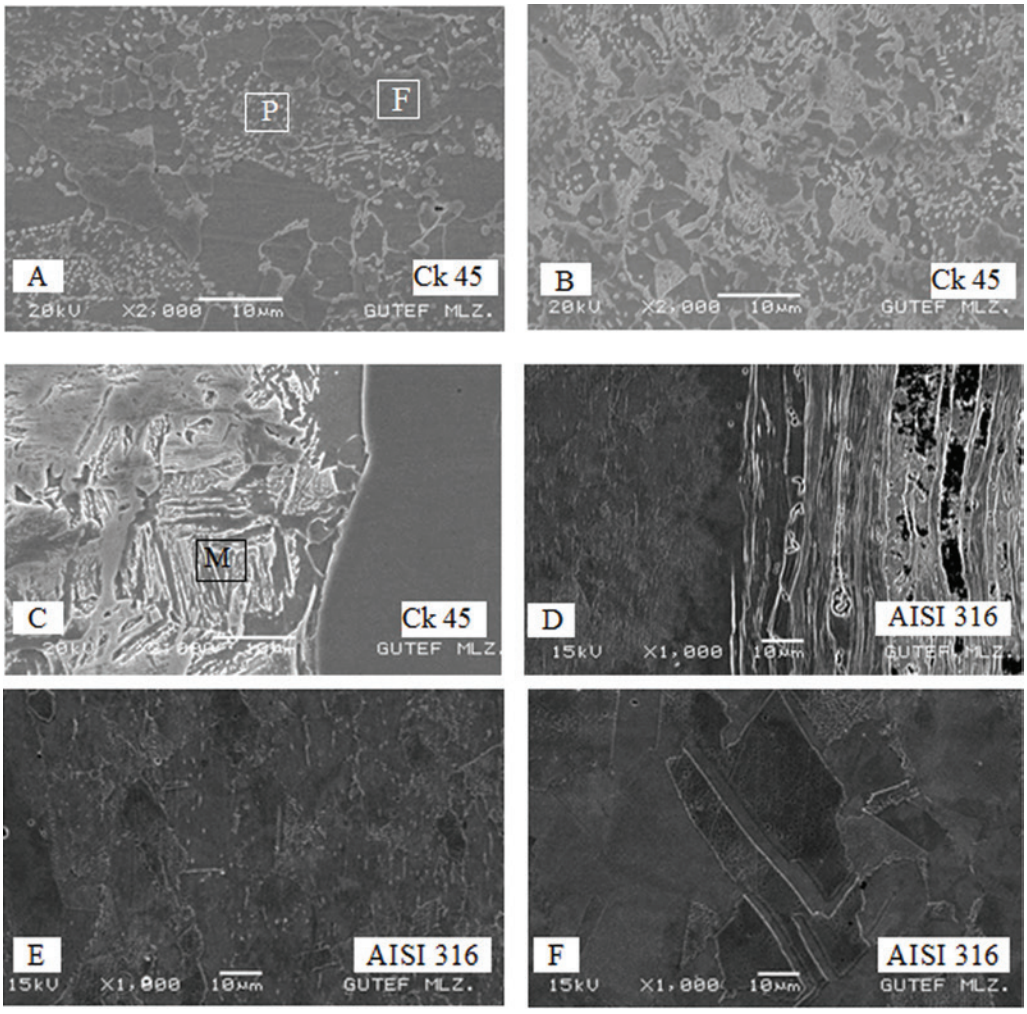

Fig. 7: FESEM microstructures of welded specimen in the different zones

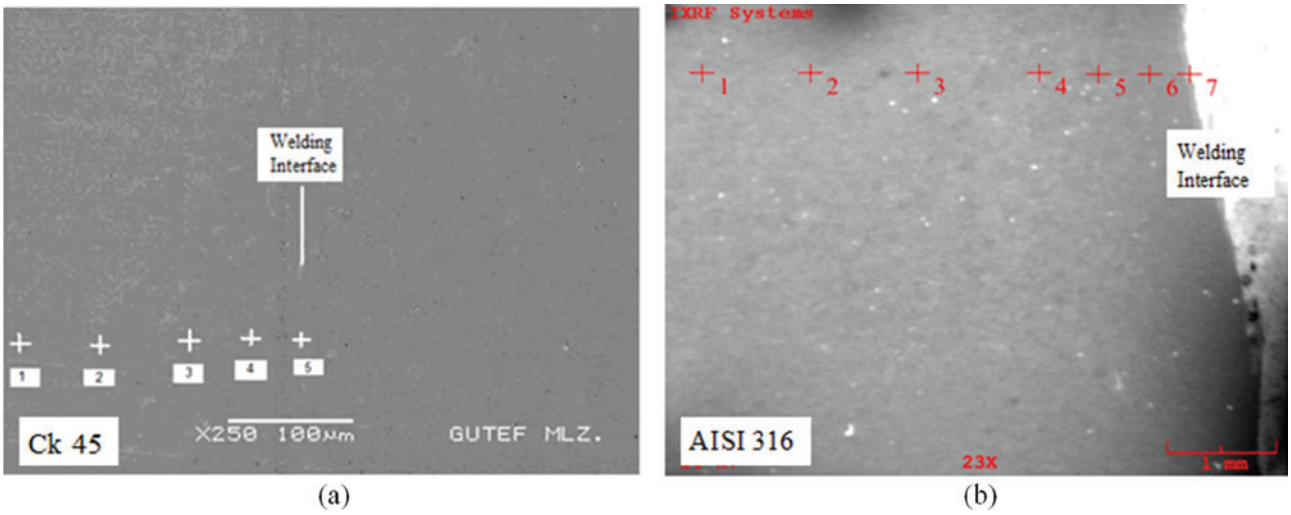

Fig. 8: EDS points of sample 13's FESEM taken by (a) Ck 45, (b) AISI 316

Table 5: EDS data of Ck 45 steel for sample 13

Element %	1	2	3	4	5
Cr	1,511	1,059	2,313	1,767	6,821
Mn	0,337	1,893	2,869	2,410	1,639
Fe	92,574	92,718	85,684	90,351	78,788
Ni	3,569	3,364	5,382	4,079	7,069
Mo	2,008	0,965	3,752	1,394	5,683

Fig. 9: The macroscopic view of tensile tested sample

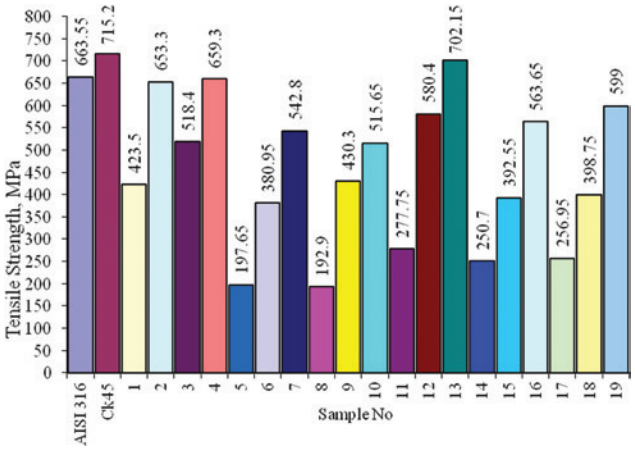

Fig. 10: Average tensile strength values of welded specimens and parent materials

the change of hardness fails to occur frequently due to the lack of heat change and phase transformation in the austenitic stainless steel. The hardness distribution stand in parallel with the structural changes (Figure 5).

Table 6: EDS data of AISI 316 steel for sample 13

Element %	1	2	3	4	5	6	7
Cr	18,530	17,193	19,358	16,395	19,370	17,870	15,235
Mn	3,181	2,091	3,125	4,844	2,274	3,360	4,583
Fe	55,975	63,176	63,792	62,981	56,553	57,647	62,205
Ni	15,951	9,670	8,869	11,026	14,617	15,240	12,451
Mo	6,363	2,651	4,856	4,754	7,187	5,882	5,526

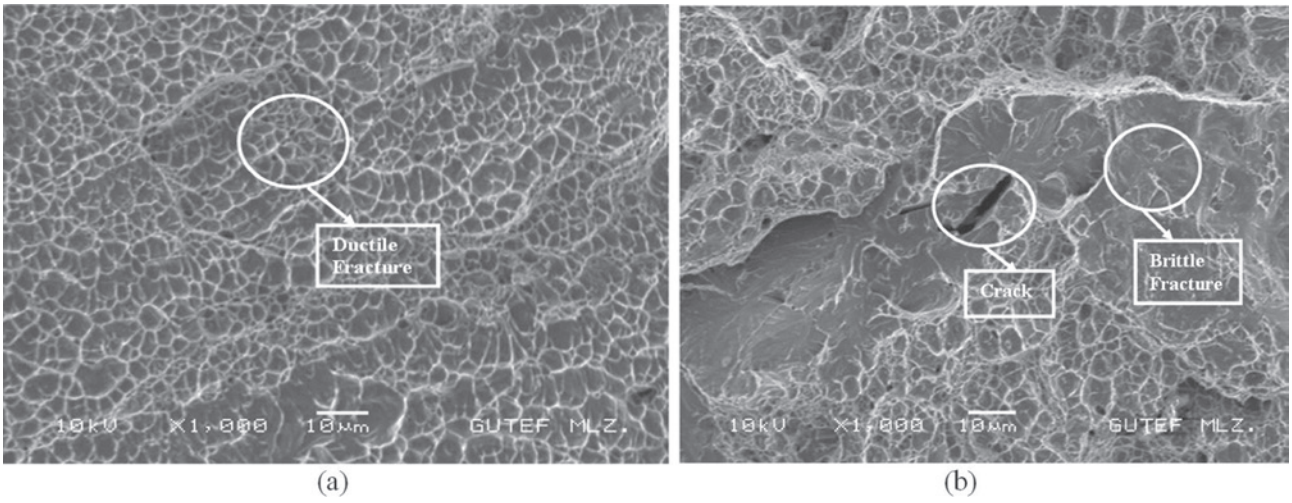

Fig. 11: FESEM images of the tensile fracture surfaces of (a) sample 13 and (b) sample 8

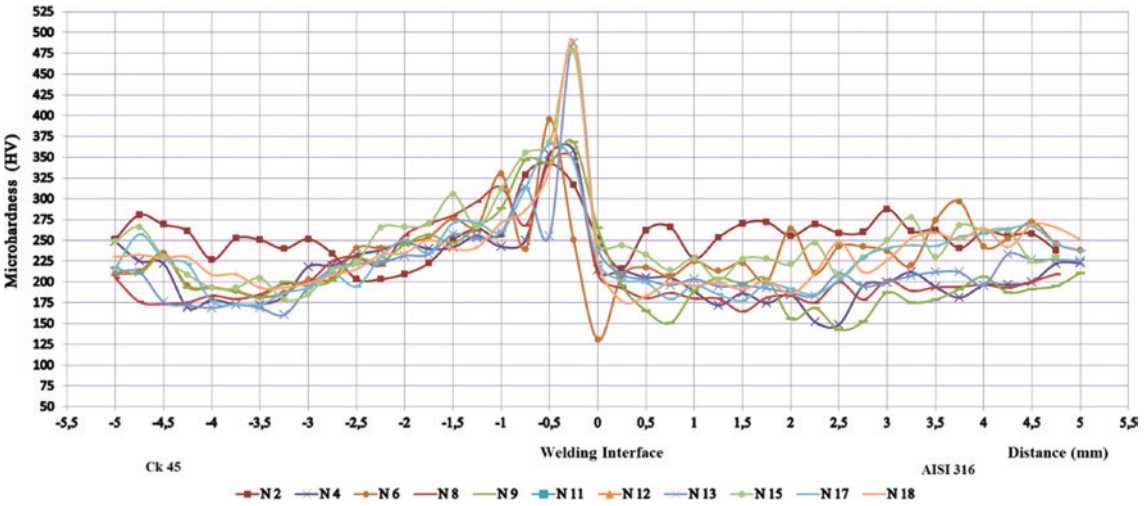

Fig. 12: Hardness variations on horizontal distance

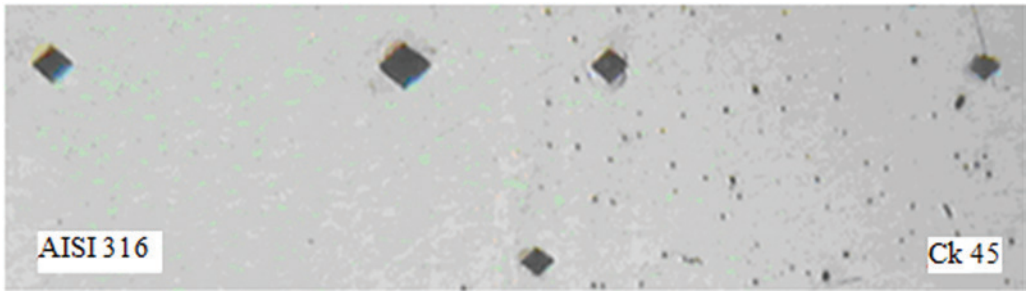

Fig. 13: Optical microstructure image of hardness traces of welded sample (25×)

4 Conclusion

The considerable results obtained by the study are summarized as follows:

The joining of AISI 316 and Ck 45 steels has been achieved by using the friction welding method.

As a result of the optical and FESEM microstructure analysis, it is realized the dynamic re-crystallization and new grain structure occur in the HAZ of AISI 316 steel. The size of this grain structure changes in accordance with the heat and deformation amount (axial pressure and hot torsion). The small grain size in the areas close to the welding interface is enlarged in sections directed towards the main material. On the other hand, the formation of martensite structure is observed in the areas close to the welding interface in the HAZ of Ck 45 steel.

In the EDS analysis of the welding area, the Fe rate is decreased in the side of Ck 45 steel whereas the Cr, Ni and Mo rates are increased. On the other hand, the Fe rate is increased in the side of AISI 316 steel while the Cr, Ni and Mo rates are decreased.

In the results of tensile tests, the lowest tensile rate is achieved as 192.9 MPa whereas the highest tensile rate is achieved as 702.15 MPa. Considering the highest tensile rate, 5.8% more tensile strength has been achieved with regard to the AISI 316 steel (tensile strength = 663.53 MPa). By the analysis of fracture surface, it is observed the fracture exists in the Ck 45 steel side of the welding area.

In the conducted hardness test, the hardness value has shown rapid increase within the first 1 mm range from the welding area towards the Ck 45 steel whereas the reason for this case has been associated with the formation of martensite structure. From the welding area to the AISI 316 steel side, it has been observed the hardness value fails to change generally.

It is realized the most effective welding parameters in the welding process of AISI 316 and Ck 45 steels are the friction time (t_s) and the upset pressure (P_u). The increase of upset pressure is in direct proportion with the increase of tensile strength. It is also stated the cracks might occur on the welding interface while the upset pressure is set low.

In the friction welding of AISI 316 and Ck 45 steels, the optimum welding parameters are 200 MPa upset pressure with 20 s of upset time in the 3000 rev/min rotational speed with 100 MPa friction pressure and 10 s of friction time.

Received: May 6, 2013. Accepted: July 19, 2013.

References

[1] S.D. Meshram, T. Mohandas, G. Madhusudhan Reddy, *J. Materials Processing Technology,* **184**, 330–337 (2008).
[2] Welding Handbook, *Welding Processes*, **2**, Eighth edition, Copyright by the American Welding Society Inc., Miami, pp. 739–761 (1997).
[3] R.E. Chalmers, *Manufacturing Engineering,* **126**, 64–65 (2001).
[4] D.E. Spindler, *Welding Journal*, 37–42 (1994).
[5] H.E. Boyer, T.L. Gall, *Joining, Metals Handbook*, Desk Edition, Metals Park, Ohio 44073, pp. 30–58 (1988).
[6] P. Jenning, *The Welding Institute*, Abinghton Hall Cambridge, pp. 147–153 (1971).
[7] P. Sathiya, S. Aravindan, A.H. Noorul, *Materials and Design*, **29**, 1099–1109 (2007).
[8] M.B. Uday, M.N. Ahmad Fauzi, H. Zuhailawati, A.B. Ismail, *Science and Technology of Welding and Joining*, **15**(7), 534–558 (2010).
[9] M.N.A. Fauzi, M.B. Uday, H. Zuhailawati, A.B. Ismail, *Materials and Design*, **31**, 670–676 (2010).
[10] N. Arivazhagan, S. Singh, S. Prakash, G.M. Reddyb, *Materials Science and Engineering B*, **132**, 222–227 (2006).
[11] J. Domblesky, F.F. Kraft, *Journal of Materials Processing Technology*, **191**, 82–86 (2007).
[12] C.J. Cheng, *Welding Journal,* **41**(12), 524–550 (1962).
[13] S. Celik, I. Ersözlü, *Materials and Design*, **30**, 970–976 (2009).
[14] M. El Wahabi, J.M. Cabrera, J.M. Prado, *Materials Science and Engineering A*, **343**, 116–125 (2003).
[15] N. Özdemir, F. Sarsılmaz, A. Hasçalık, *Materials and Design*, **28**, 301–307 (2007).
[16] M. Sahin, *Materials and Design*, **28,** 2244–2250 (2007).
[17] S. Celik, D. Dinc, R. Yaman, I. Ay, *Practical Metallography*, **47**(4), 188–204 (2010).
[18] N. Arivazhagan, S. Singh, S. Prakash, G.M. Reddyb, *Materials and Design*, **32**, 3036–3050 (2011).
[19] M.G. Reddy, S.A. Rao, T. Mohandas, *Science and Technology of Welding & Joining*, **13**(7), 619–628 (2008).
[20] G. Krauss, *ASM International Materials Park*, Ohio, pp. 141–145, 495–531 (2005).
[21] B.L. Bramfitt, A.O. Benscoter, *ASM International Materials Park*, Ohio (2002).
[22] S.A.A. Akbarimousavi, M. Gohari Kia, *Materials and Design*, **32**, 3066–3075 (2011).
[23] I. Bhamji, M. Preuss, P.L. Threadgill, R.J. Moat, A.C. Addison, M.J. Peel, *Materials Science and Engineering A*, **528,** 680–690 (2010).
[24] S. Kim, Y.C. Yoo, *Materials Science and Engineering A*, **311**, 108–113 (2001).